EFDA–JET–CP(10)08/11

R. De Angelis, F. Orsitto, M. Baruzzo, P. Buratti, B. Alper, L. Barrera,
A. Botrugno, M. Brix, K. Crombé, L. Figini, A. Fonseca, C. Giroud,
N. Hawkes, D. Howell, E. De La Luna, V. Pericoli, E. Rachlew,
O. Tudisco and JET EFDA contributors

Determination of q Profiles in JET by Consistency of Motional Stark Effect and MHD Mode Localization

Determination of q Profiles in JET by Consistency of Motional Stark Effect and MHD Mode Localization

R. De Angelis[1], F. Orsitto[1], M. Baruzzo[2], P. Buratti[1], B. Alper[3], L. Barrera[4], A. Botrugno[1], M. Brix[3], K. Crombé[4], L. Figini[6], A. Fonseca[7], C. Giroud[3], N. Hawkes[3], D. Howell[3], E. De La Luna[5], V. Pericoli[1], E. Rachlew[8], O. Tudisco[1] and JET EFDA contributors*

JET-EFDA, Culham Science Centre, OX14 3DB, Abingdon, UK

[1]*Associazione Euratom/ENEA sulla Fusione, CP 65-00044 Frascati, Rome, Italy*
[2]*Consorzio RFX, EURATOM-ENEA Association, Corso Stati Uniti 4, 35127 Padova, Italy*
[3]*EURATOM/UKAEA Fusion Association, Culham Science Centre, Abingdon, OX14 3DB, UK*
[4]*Department of Applied Physics, Ghent University, J. Plateaustraat 44, 9000 Gent, Belgium*
[5]*Laboratorio Nacional de Fusión, Asociación EURATOM-CIEMAT, 28040, Madrid, Spain*
[6]*Istituto di Fisica del Plasma, Associazione EURATOM ENEA -CNR,Milano, Italy*
[7]*Associacao Euratom-IST,Centro de Fusao Nuclear, Av. Rovisco Pais,Lisbon, Portugal*
[8]*Association EURATOM-VR,KTH Royal Inst. of Technology,SE-10691Stockholm, Sweden*
** See annex of F. Romanelli et al, "Overview of JET Results", (23rd IAEA Fusion Energy Conference, Daejon, Republic of Korea (2010)).*

Preprint of Paper to be submitted for publication in Proceedings of the 23rd IAEA Fusion Energy Conference, Daejon, Republic of Korea (10th October 2010 - 16th October 2010)

ABSTRACT.
The measurement of the safety factor q in tokamaks, which describes the winding of the helical magnetic field lines, is very important especially for the achievements of advanced scenarios. The motional Stark effect diagnostic can provide a direct measurement of the magnetic field orientation but the derivation of the q-profiles requires a simulation of the magnetic equilibrium taking into account inputs from several other diagnostics. This analysis can be affected by large errors. In order to validate the results, q profiles are compared with the radii of MHD modes, which can be attributed to surfaces of known q. This paper analyses the errors in the assumptions on the derivation of the MHD mode localization.

1. INTRODUCTION

The performances of Advanced Tokamak (AT) [1] scenarios depend substantially on the radial behaviour of the safety factor $q = rB_t/RB_p$, (where r and R are the minor and major radii, and B_t and B_p are the toroidal and poloidal magnetic fields). The direct measurement of q is a challenging diagnostic issue, due to the inaccessibility of high temperature plasma regions to material probes. Significant information can be obtained by the MSE (Motional Stark Effect) diagnostic, which measures the direction of the local magnetic field by the polarimetry of radiation emitted by fast neutral beams. Information on the radial q-profile can also be extracted by the study of magnetic islands, characterized by toroidal (n) and poloidal (m) mode numbers, which resonate on surfaces where $q = m/n$. A previous work [2,3] reported the results of comparisons of MSE q profiles in JET discharges [4,5] with the radial locations of MHD modes [6, 7], which appeared quite satisfactory for monotonic profiles. The radius of a magnetic island can be obtained as the location where the island rotation frequency matches the ion diamagnetic frequency profile in the frame with zero radial electric field ($\omega = \omega^*_i + \omega_{E\times B}$). Alternatively the island radius can be identified as the position where the temperature oscillation exhibits a π phase jump. The present paper analyses the assumptions and limits implicit in the estimation of the rotation frequency. On the other hand for reversed q profiles (minimum of q(r) not in the plasma centre) the reconstruction from MSE data is more uncertain, and the localization of MHD is also more difficult due to uncertainty in the m number. The profile reversal is often marked by other well identifiable MHD activity (Alfvén Cascades) [8,9] that starts when the minimum q is at an integer or half integer value.

2. MEASUREMENT OF THE Q PROFILE

The equilibrium magnetic field in tokamak lies on nested toroidal surfaces that enclose constant values of both toroidal and poloidal magnetic fluxes. The safety factor q, which represents the thread of the helical magnetic field lines winding around the torus, is given by the derivative of toroidal flux with respect to the poloidal one. At the periphery of the plasma, magnetic coils can measure the shape and q value of magnetic surfaces quite accurately. Conversely, the measurement of these quantities inside the hot plasma is hindered by the impossibility of using physical probes. A

full description of the radial magnetic equilibrium can be obtained by solving the Grad-Shafranov equation [7], describing the plasma pressure balance, with the peripheral boundary condition; however this approximation leads to large uncertainties in the plasma core. In a well-diagnosed tokamak, there are several diagnostic inputs, which can be used to constrain or supplement the equilibrium simulation: namely LIDAR, Thomson Scattering, Core Spectroscopy and ECE (Electron Cyclotron Emission) provide profiles of the electron and ion temperatures and densities to evaluate the kinetic pressure; while some knowledge of the local magnetic field and plasma rotation is also available from Faraday rotation and Charge exchange spectroscopy. The most relevant contribution to the description of the magnetic equilibrium is obtained from the Motional Stark Effect diagnostic (MSE), which measures directly the pitch angle of magnetic field lines. This technique relies on the observation of the D_α line emitted by the fast neutral Deuterium atoms injected in most tokamaks for additional heating. Due to the high electric field experienced by the particles moving in the magnetic field, one of the Stark-split components of the H_α line is polarized in the direction of the magnetic field. Polarimetric measurements [10,11] can thus provide the local magnetic field orientation at the intersection of the line of sight with the beam. A typical layout for the MSE diagnostic is illustrated in Fig.1.

The accuracy of this technique is very high although it can be hampered by the presence of background polarized radiation. The radial positions for the MSE data points and a typical magnetic configuration in the JET tokamak are illustrated in Fig.2.

Although the MSE polarization angles can be measured precisely, they do not determine independently the shape of the plasma magnetic surfaces. As a consequence, MSE data can be used more profitably as constraints to magnetic equilibrium reconstruction codes. Equilibrium simulations including constraints from the diagnostics listed above give better descriptions of the magnetic surfaces and of q profiles.

3. LOCALIZATION OF MAGNETIC ISLANDS

Magnetic islands originated by tearing instabilities [7] give rise to magnetic oscillations, which can be detected by Mirnov coils at the plasma edge. These oscillations are characterized by toroidal (n) and poloidal (m) mode numbers, associated to the mode periodicity in the torus angles, and correspond to rational q=m/n values resonating with the island helicity. Mode identification is obtained by Fourier analysis of the signals and phase comparison between coils at different locations. This leads to a clear attribution of the n number, while the m number is subject to a degree of arbitrariness.

The radial localization of the island has been obtained following two independent methods:

3.1. TEMPERATURE OSCILLATIONS

Magnetic islands induce temperature oscillations inside the plasma. Temperature signals from ECE radiometer are cross-correlated with a reference signal from a Mirnov coil, so that amplitude, phase and coherence are obtained as a function of the plasma major radius. In particular, the radial phase

profile shows a π jump whenever an island is crossed, moving along the radial coordinate.

Figure 4 illustrates a comparison of MHD markers obtained from ECE and from the island velocity.

3.2. ISLAND ROTATION FREQUENCY

The island location is given by the radius at which the measured island frequency matches the ion diamagnetic frequency profile in the frame with zero radial electric field, i.e. $\omega = \omega^*_i + \omega_{E\times B}$. Profiles of $\omega^*_{i,}$ and $\omega_{E\times B}$ are calculated from ion temperature and rotation as measured by Charge Exchange Spectroscopy at different radii. In the hypothesis that the mode rotates with the plasma fluid, the island rotation frequency can be expressed as [12, 14] :

$$\omega = n\left(\Omega_{C\phi} - \frac{5}{6}\frac{\partial T_{C)}}{\partial\psi}\right) + k_\theta v_{C\theta} - n\frac{\partial(T_i - T_C)}{\partial\psi} + \frac{nT_C}{6}\frac{\partial 1\mathrm{n}\, N_i}{\partial\psi} - nT_i\frac{\partial 1\mathrm{n}\, N_i}{\partial\psi} \qquad (1)$$

Where

Ω_{Cf} = *Carbon toroidal rotation frequency*
v_{CJ} = *Carbon Poloidal velocity*
T_C = *Ion Temperature, Carbon*
T_i, N_i = *Deuterium Ion Temperature, Density*
y = *Magnetic flux*
k_J = *Island poloidal wave number*

On a first approximation in the equation above, only the first two terms have been considered. A typical result is shown in Fig. 5, where the markers from MHD analysis (the figure reports modes with m/n = 1/1,4/3,3/2) are compared with EFIT profiles with and without MSE conditioning) and in Fig.6 which shows the time behaviour of the radius of the q = 1.5 surface from the equilibrium and from MHD.

The comparison has been extended to all shots of the experimental campaign in the Hybrid scenario [12,13], characterized by monotonic profiles. The database includes 1600 time steps in 225 shots. The difference on the radii of the q=1.5 surface gives an average error $(R_{MSE} - R_{MHD})/R_{MHD}$ which is reduced from ~ 8% to ~ 1.5% when using the diamagnetic correction as illustrated in Fig.7.

4. FULL EVALUATION OF THE TERMS CONTRIBUTING TO THE ISLAND ROTATION FREQUENCY

In order to understand the accuracy of the results above, we are now considering all terms in equation 1. Data for the Carbon Temperature and velocity are taken from charge exchange spectroscopy, in the hypothesis that $T_i = T_c$ and $N_i = n_e/Z_{eff}$.

In figure 8 the horizontal dotted line corresponds to the frequency measured by Mirnov coils. The island radius is evaluated by the intersection with the curves representing the various approximations to equation 1.

It can be noticed that the island radius moves outward when moving form the curve $\omega = n \cdot \Omega_{C\phi}$ o the curve $\omega = n \left(\Omega_{C\phi} - \frac{5}{6} \frac{\partial T_{Ci}}{\partial \psi} \right)$, this corresponds to the results illustrated in the previous paragraph. The remaining terms are strongly dominated by the $k_\vartheta v_{C\vartheta}$ contribution. In particular there is a significant difference in using the measured $v_{C\vartheta}$ or the value estimated with the neoclassical approximation (see fig.9). Even in the internal region (close to the q =3/2 surface), the difference in the two values is high enough to produce a substantial agreement with the MSE profile only when $v_{C\vartheta} << v_{C\vartheta}^{CXRS}$. The difference cannot be accounted for by the inclusion of the error bar in the velocity measurement: in Fig.10 the terms related with the upper bound (green circles) and lower bound (magenta circles) on the $k_\vartheta v_{C\vartheta}$ are shown.

5. PROFILES WITH SHEAR REVERSAL

The analysis of q-profiles with a minimum off the plasma centre can lead to higher uncertainties in the identification of the rational surfaces. In some cases the identification of internal modes by X ray tomography, can help to describe the reversed region. An example is shown in Fig.11.

In reversed shear discharges it also possible to observe fast sequences of modes with varying m numbers (Alfvén Cascades-AC) when q_{min} passes through a rational value. This effect is used in the calibration of q_{MSE} in dedicated shots. The time coincidence between AC's and $q_{min}^{rational}$ has been checked in set of 30 shots with different characteristics showing that the calibration grossly holds in about 90% of the cases with time uncertainties less than 0.5 s. FIG.12 illustrates the q_{MSE} profiles at the crossing of the q = 3 and q = 2 on the same shot.

CONCLUSION

In JET hybrid discharges, the profiles of the safety factor q show a good agreement with markers obtained from MHD analysis. The agreement holds if the rotation velocity of the island is evaluated either by neglecting the poloidal velocity or using a value close to the neo-classical approximation (e.g. much smaller than the experimental one). The model used implies that the mode rotates rigidly with the plasma. Some more investigation is needed to understand the physical limits of this hypothesis.

For reversed profiles, uncertainties in q values near the axis are higher than those for monotonic profiles, although in some cases they are seen to correspond with experimental data from X- ray tomography and with the observation of Alfvén Cascades.

REFERENCES:

[1]. C.M. Greenfield et al. Plasma Physics and Controlled Fusion **46** (2004); doi:10.1088/0741-3335/46/12B/019

[2]. R. De Angelis et al., Nuclear Instruments and Methods A (2010); doi:10.1016/j.nima.2010.04.151
[3]. R. De Angelis et al. 36th EPS Conf. on Plasma Phys.Sofia (2009)
[4]. M. Brix, et al. Review of Scientific Instruments **79**, 10F325 (2008); doi:10.1063/1.2964180
[5]. M.A. Makoski et al. 35th EPS Conf. on Plasma Physics ECA Vol 32D, P-4.085 (2008)
[6]. G. Bateman "MHD instabilities" MIT Press, Cambridge, Mass. (1978)
[7]. J. Wesson - Tokamaks 2nd ed. Oxford Science Pubbl. 1997
[8]. S. Sharapov et al. Phys. Plasmas 9, 2027 (2002); doi:10.1063/1.144834
[9]. S. Hacquin et al. PPCF 49 (2007) 1371-1390; doi:10.1088/0741-3335/49/9/002
[10]. F. De Marco, S. Segre – Plasma Physics **14** 245 (1972)
[11]. I.H. Hutchinson – Principles of plasma diagnostics Cambridge University Press (1987)
[12]. P. Buratti et al. 36th EPS Conf. on Plasma Phys. Sofia (2009)
[13]. J. Hobirg et al. 36th EPS Conf. on Plasma Phys. Sofia (2009)
[14]. R.J. La Haye et al. Physics of Plasmas **10**, 3644 (2003); doi:10.1063/1.1602452

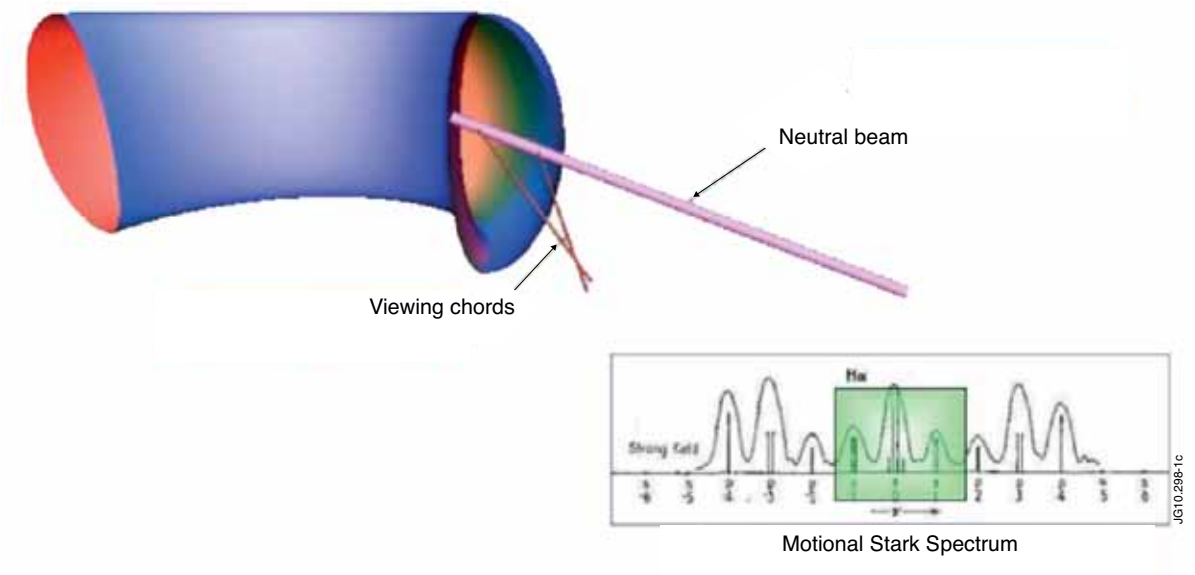

Figure 1: Schematics of the MSE diagnostic.

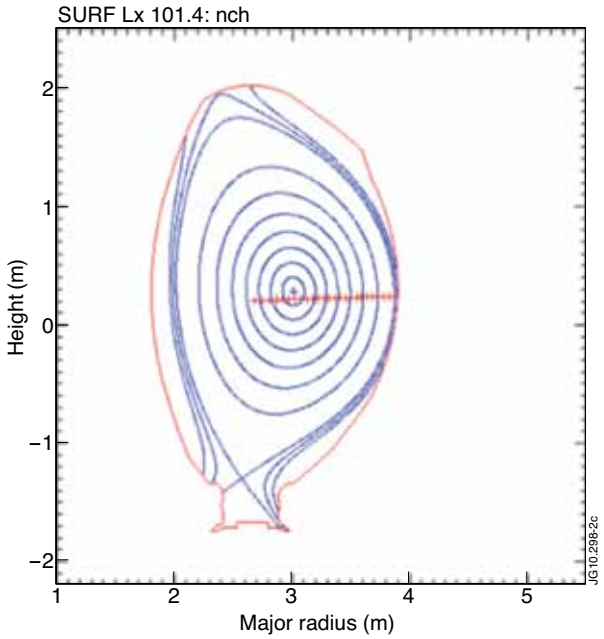

Figure 2: Typical flux surfaces in JET and MSE measuring points.

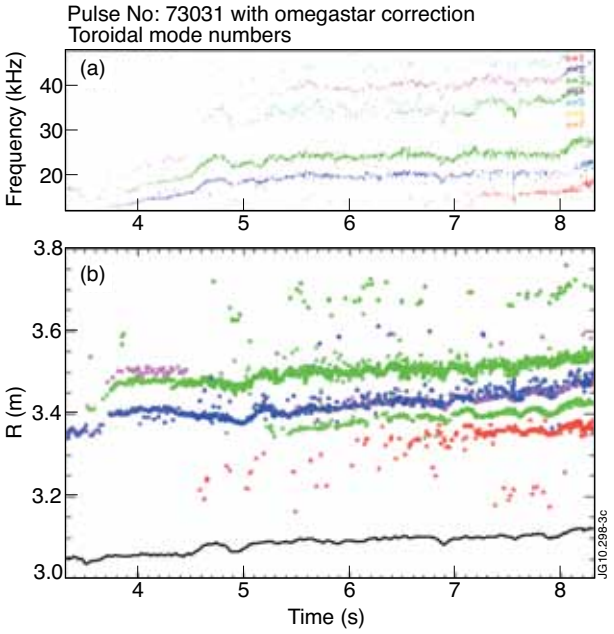

Figure 3: Mode frequency and mode location.

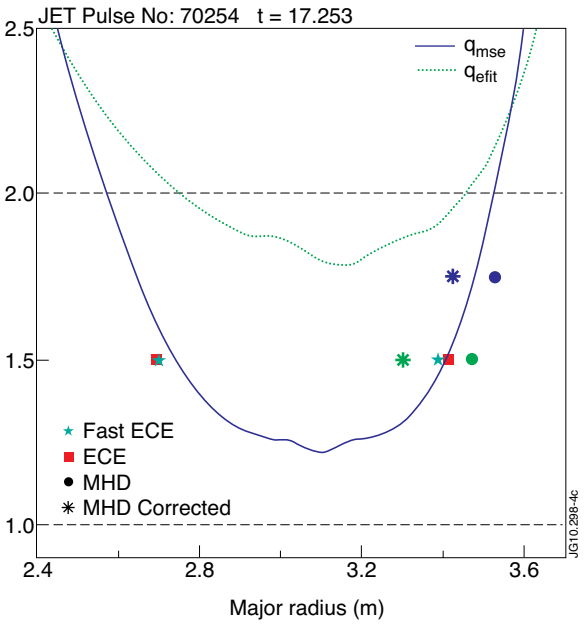

Figure 4: Comparison of q profiles with data from ECE The continuous curves represent the profiles obtained from the EFIT equilibrium calculation without (q_{EFIT}) and with (q_{MSE}) MSE -polarimetry-constraints.
Markers are obtained by different island localization methods:
1) Temperature oscillations (ECE and Fast ECE);
2) Island rotation velocity (MHD and MHD corrected, see next paragraph)

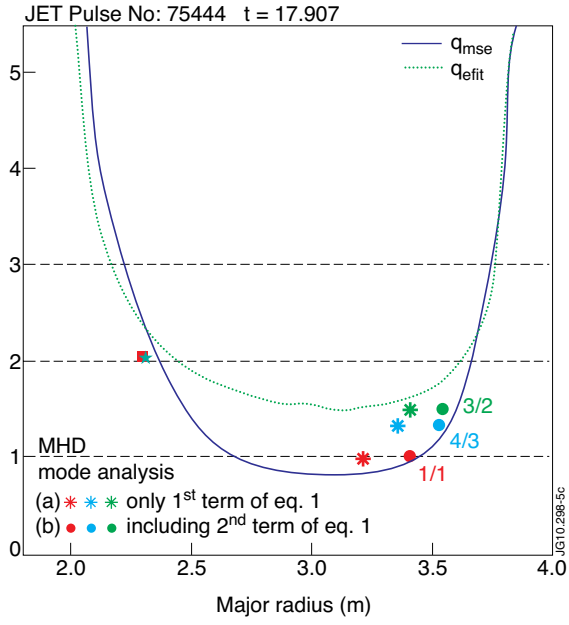

Figure 5: Behaviour of q versus major radius. From EFIT: q_{EFIT}-unconstrained equilibrium; q_{MSE} with MSE and total pressure constraints. From MHD analysis:
- ✶ *MHD – only 1st term in eq.1,*
- ● *MHD corrected including 2nd term in eq.1.*

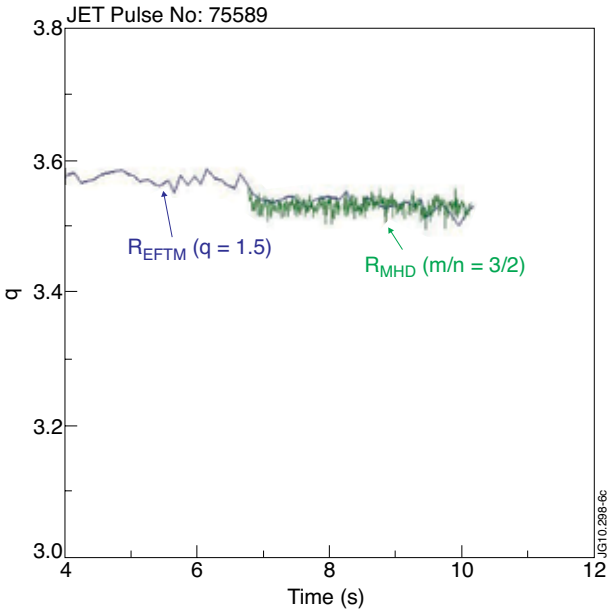

Figure 6: Time behaviour of the radii of the q = 3/2 and q = 5/2 from MHD analysis and from the EFIT reconstruction.

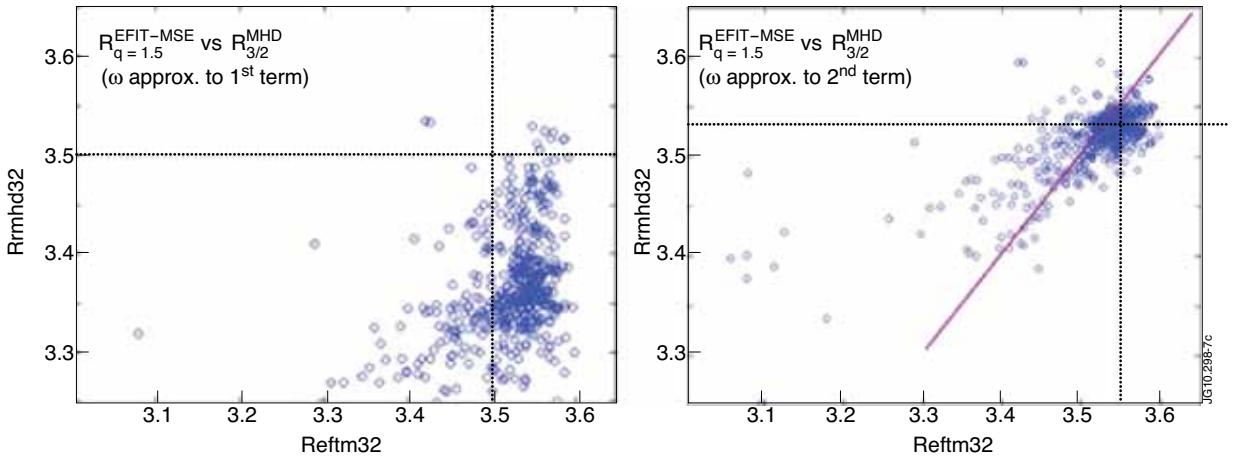

Figure 7: The radii of the q = 1.5 surface from the MSE constrained EFIT and from MHD location of the m/n = 3/2 radial location. Case a) and b) of Fig.5.

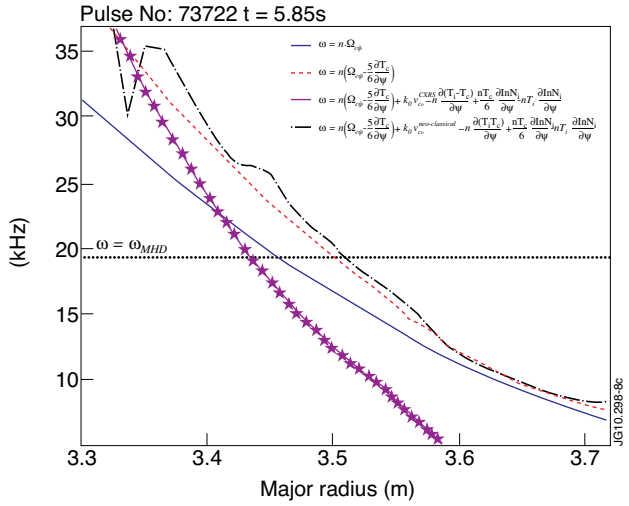

Figure 8: Illustration of the influence of terms in equation1

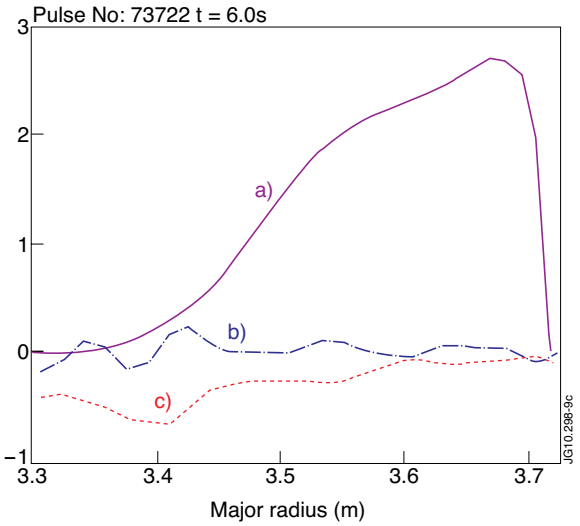

Figure 9:Comparison of poloidal velocities

v_{θ}^{Carbon} *measured (CXRS)*
v_{θ}^{Carbon} *neo-classical (JETTO)*
$v_{\theta}^{Deuterium}$ *neo-classical (JETTO)*

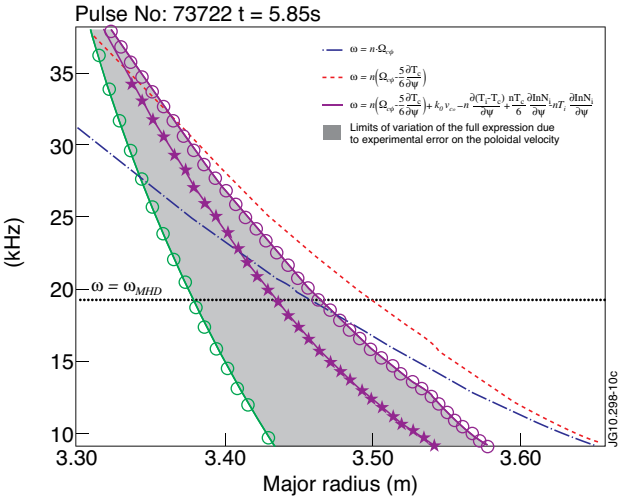

Figure 10: Effect of the experimental error on v^{CXRS}

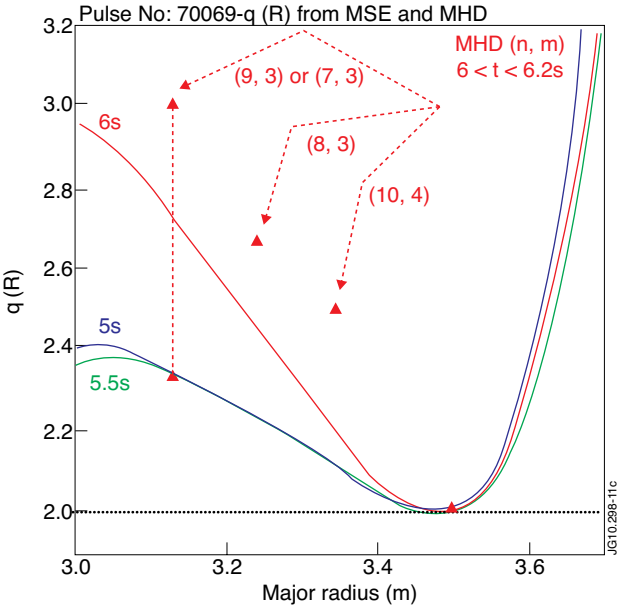

Figure 11: Comparison of q_{MSE} *and internal modes localisation by X-ray tomography.*

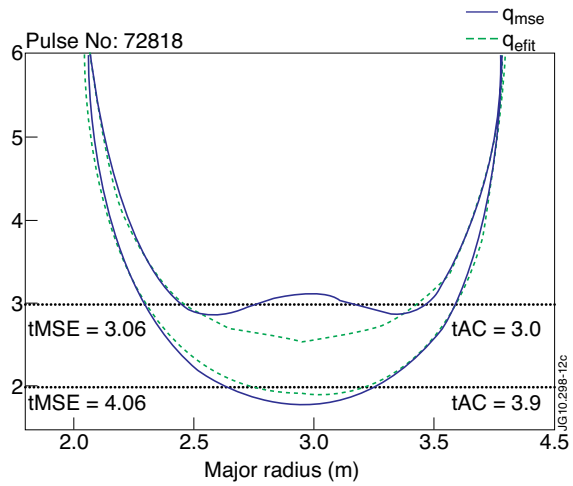

Figure 12: q-profiles at the crossing of the q_{min}*=3 and* q_{min}*=2 surfaces*